

Regional climate change experiments over southern South America. II: Climate change scenarios in the late twenty-first century

Mario N. Nuñez · Silvina A. Solman ·
Maria Fernanda Cabré

Received: 20 December 2007 / Accepted: 14 July 2008
© Springer-Verlag 2008

Abstract We present an analysis of climate change over southern South America as simulated by a regional climate model. The regional model MM5 was nested within time-slice global atmospheric model experiments conducted by the HadAM3H model. The simulations cover a 10-year period representing present-day climate (1981–1990) and two future scenarios for the SRESA2 and B2 emission scenarios for the period 2081–2090. There are a few quantitative differences between the two regional scenarios. The simulated changes are larger for the A2 than the B2 scenario, although with few qualitative differences. For the two regional scenarios, the warming in southern Brazil, Paraguay, Bolivia and northeastern Argentina is particularly large in spring. Over the western coast of South America both scenarios project a general decrease in precipitation. Both the A2 and B2 simulations show a general increase in precipitation in northern and central Argentina especially in summer and fall and a general decrease in precipitation in winter and spring. In fall the simulations agree on a general decrease in precipitation in southern Brazil. This reflects changes in the atmospheric circulation

during winter and spring. Changes in mean sea level pressure show a cell of increasing pressure centered somewhere in the southern Atlantic Ocean and southern Pacific Ocean, mainly during summer and fall in the Atlantic and in spring in the Pacific. In relation to the pressure distribution in the control run, this indicates a southward extension of the summer mean Atlantic and Pacific subtropical highs.

Keywords Regional climate modeling · Southern South America · Climate change scenarios

Abbreviation

RCM	Regional climate model
AGCM	Atmospheric general circulation model
AOGCM	Atmospheric-ocean general circulation model
SLP	Sea level pressure
DJF	December-January-February
MAM	March-April-May
JJA	June-July-August
SON	September-October-November

M. N. Nuñez (✉) · S. A. Solman
Centro de Investigaciones del Mar y la Atmósfera
(CIMA-CONICET/UBA) DCAO (FCEyN-UBA),
Ciudad Universitaria, Pabellón II,
Piso 2, 1428 Buenos Aires, Argentina
e-mail: mnunez@cima.fcen.uba.ar

S. A. Solman
e-mail: solman@cima.fcen.uba.ar

M. F. Cabré
Centro de Investigaciones del Mar y la Atmósfera
(CIMA-CONICET/UBA), Ciudad Universitaria, Pabellón II,
Piso 2, 1428 Buenos Aires, Argentina
e-mail: cabre@cima.fcen.uba.ar

1 Introduction

The Second National Communication of Argentina for Climate Change aimed to advance the climate impact research for the region. In this context, climate change simulations of southern South America climate were performed using a regional climate model (RCM) nested in time slice atmospheric general circulation model (AGCM) experiments.

In a companion paper by Solman et al. (2008) (hereafter referred to as SNC) we have presented an evaluation of the

present climate simulation performed with a RCM nested within an AOGCM, covering the period 1981–1990. In this paper we analyze two 10-year scenario simulations performed for the period 2081–2090, one for the SRESA2 and the other for the SRESB2 emission scenario (IPCC 2000). The regional model used in both, SNC and the present work, is the Fifth-generation Pennsylvania-State University-NCAR non-hydrostatic Mesoscale Model MM5 (Grell et al. 1993) version 3.6. The large scale fields used to drive the MM5 simulations were obtained from corresponding time slice experiments with the global atmospheric model HadAM3H (Pope et al. 2000). The length of the simulations is 10 years to give a reasonable idea of the mean climate change. Certainly 10 years is a minimum that allows obtaining some information of at least some aspects of climate change.

We investigate the annual and seasonal average change in climatic variables and the change in the annual cycle. This study represents a new focus area (South America) within the context of nested regional climate simulations. Previously, RCM experiments have become available mainly for the European region, as part of the PRUDENCE project (Christensen et al. 2007), North America, as part of the North American Regional Climate Change Assessment Program (Mearns et al. 2005) and Australia (Whetton et al. 2001).

The focus here is on the simulated climate changes; in particular those in surface temperature and precipitation, the two variables most used in impact assessment studies. Nevertheless, we also examine the changes in the sea level pressure and in the circulation structure to better understand the surface climate change signal. Our analysis is based on the seasonal mean conditions, aspects of the annual cycle and extreme precipitation events. The present climate simulation (1981–1990) was analyzed in detail in SNC, and is not discussed here. The regional changes projected for the A2 and B2 experiments are intercompared to examine how the regional climate change pattern depends on the greenhouse gases forcing scenarios.

2 Model and experiment design

The regional climate model used for the present study is the Fifth-generation Pennsylvania-State University-NCAR non-hydrostatic Mesoscale Model MM5 (Grell et al. 1993) version 3.6. The model grid interval is 50 km (average), and its domain covers southern South America and surrounding oceans, to avoid the lateral boundary conditions being over the complex topography of the region. The model configuration is the same as in SNC.

The experiment design follows Jones et al. (2001): The HadAM3H model drives the corresponding MM5

experiment for the period 1981–1990. For the simulation scenarios, greenhouse gas emissions are specified from the A2 and B2 emission scenarios as boundary conditions for the driving model and it drives the RCM for the time slice 2081–2090. The geopotential height, relative humidity, temperature, zonal and meridional wind components fields required as lateral boundary conditions for MM5 are taken from the global atmospheric model (HadAM3H). The variables at the boundaries are updated every 6 h, with a linear interpolation between successive updates at each MM5 time step. At sea level pressure is also updated each 6 h. The sea surface temperature and sea ice are updated monthly. The lateral meteorological boundary conditions were provided on a coarser grid than the HadAM3H one, specifically on a 2.5° latitude by 3.75° longitude grid.

As usually done in the thematic literature, we refer here to the term “change” as the difference between the selected climatic statistics in the scenario (2081–2090) and reference (1981–1990) simulation.

Figure 1 displays the model topography and domain used in this study. Most of the maps shown hereafter exclude the buffer zones and two additional rows and columns of the ordinary model area where sharp gradients in precipitation due to spurious convergence at the boundaries were found.

The present climate simulation is discussed in detail in SNC and only a few main points are repeated here. Overall, the regional MM5 model is able to capture the main features of the observed mean surface climate over southern South America, its seasonal evolution and the regional

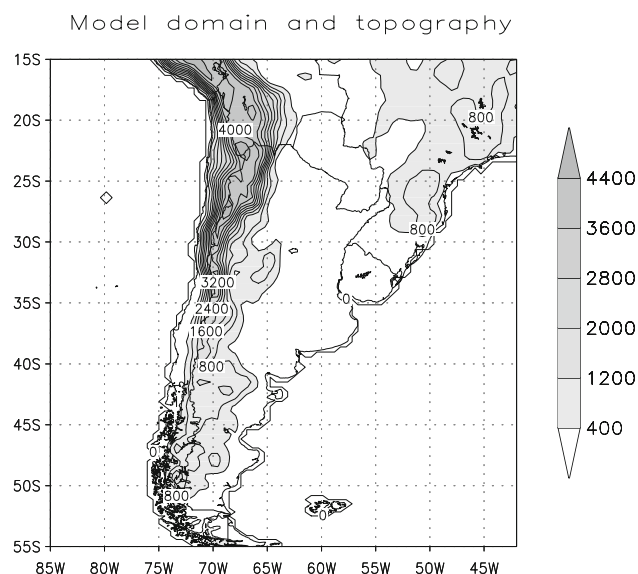


Fig. 1 Model domain and topography. Contours are drawn every 400 m. Shading represents topographic heights more than 400 m

detail due to topographic forcing. The observed regional patterns of surface air temperatures (mean, maxima and minima) are well reproduced. Biases are mostly within 3°C, temperature being overestimated over central Argentina and underestimated in mountainous regions during all seasons. Biases in northeastern Argentina and southeastern Brazil are positive during the austral spring season and negative in other seasons. In general, maximum temperatures are better represented than minimum temperatures. Warm bias is larger during the austral summer for maximum temperature and during the austral winter for minimum temperature, mainly over central Argentina.

The broad spatial pattern of precipitation and its seasonal evolution are well captured; however, the regional model overestimates the precipitation over the Andes region in all seasons and in southern Brazil during summer. Precipitation amounts are underestimated over the La Plata basin from fall to spring. Extremes of precipitation are better reproduced by the regional model compared with the driving model. Interannual variability is well reproduced too, but strongly regulated by boundary conditions, particularly during winter months.

3 Results

3.1 Changes in the mean climate

In this section changes in the 10-year seasonal, annual and monthly mean climate are analyzed. The statistical significance of the changes is addressed only for mean surface temperatures (mean, maxima and minima) and precipitation by means of a Student's *t*-test.

In general, changes for the B2 scenario are similar to those for the A2 scenario although with somewhat smaller amplitude. Nevertheless, some apparent qualitative differences arise, particularly in surface variables.

3.1.1 Mean sea level pressure and 500 hPa geopotential height

First of all we discuss the changes in large scale circulation patterns over southern South America as described by sea level pressure (SLP) and 500 hPa geopotential height fields. Changes in circulation patterns may explain some of the changes in precipitation and surface temperature, mainly because they modify the dynamical background on which the regional processes develop.

Changes in time mean sea level pressure are shown in Fig. 2 for austral summer (DJF, December-January-February), austral winter (JJA, June-July-August) and for the annual mean. Circulation changes in the HadAM3H fields are very similar to those in the regional simulation due to the

large scale forcing at the lateral boundaries, and are thus not shown. The changes in DJF are largely similar between the two scenario simulations showing a cell of increasing pressure centered in the southern Atlantic Ocean and a slight decrease in SLP over tropical and subtropical latitudes. In relation to the pressure distribution in the present climate simulation, this indicates a southward extension of the summer Atlantic and Pacific subtropical highs. The simulated changes are larger for the A2 than the B2 scenario, although with few qualitative differences. A decrease in SLP over northern Argentina, where the Chaco low is located, indicates a deepening of the low pressure system. This feature is evident in both scenarios. This pattern of change induces an increase in the northerly wind over North-eastern Argentina which is responsible of the convergence of moisture at low levels over northern Argentina, with a strong influence on the precipitation over that region, as will be discussed later. During JJA the most salient pattern of change is a decrease in SLP over tropical and subtropical regions. This behavior can be interpreted as a weakening and poleward shift of the subtropical anticyclones, as for the summer season. This behavior will have a strong influence on the projected changes in precipitation, as will be discussed later. The annual mean SLP changes suggest a marked poleward shift in the large-scale circulation patterns. This behavior is consistent with the multi-model mean changes shown in Meehl et al. (2007), where the changes of SLP projected under the A1B scenario show increases over the mid-latitude and subtropical ocean regions extending across South America during both DJF and JJA.

The change in the 500 hPa height field (Fig. 3) shows a general increase mainly due the lower tropospheric warming in the scenario simulations, which implies a thicker lower atmosphere. The structure of the pattern of change in the 500 hPa height is similar to that in the SLP field, suggesting that the climate change signal has an equivalent barotropic structure in the lower troposphere, particularly in DJF. Note the maximum increase in the geopotential height in DJF over the southern South Atlantic Ocean for both scenario simulations which induces a weakening of the north-south gradient. In consequence, westerly winds in low levels are expected to be weaker in both scenarios compared with present climate conditions (not shown). In JJA the pattern of circulation change is different, due to a maximum in the increase over subtropical latitudes, which induces an enhancement of the meridional gradient in the 500 hPa height and thus an increase in the strength of westerlies. This pattern of change is consistent with a poleward shift of the subtropical storm-track over the South Pacific and south Atlantic Oceans. The pattern of change in the geopotential height field is similar for both emission scenarios, being weaker for the B2 scenario compared with A2.

MM5 SEA LEVEL PRESSURE

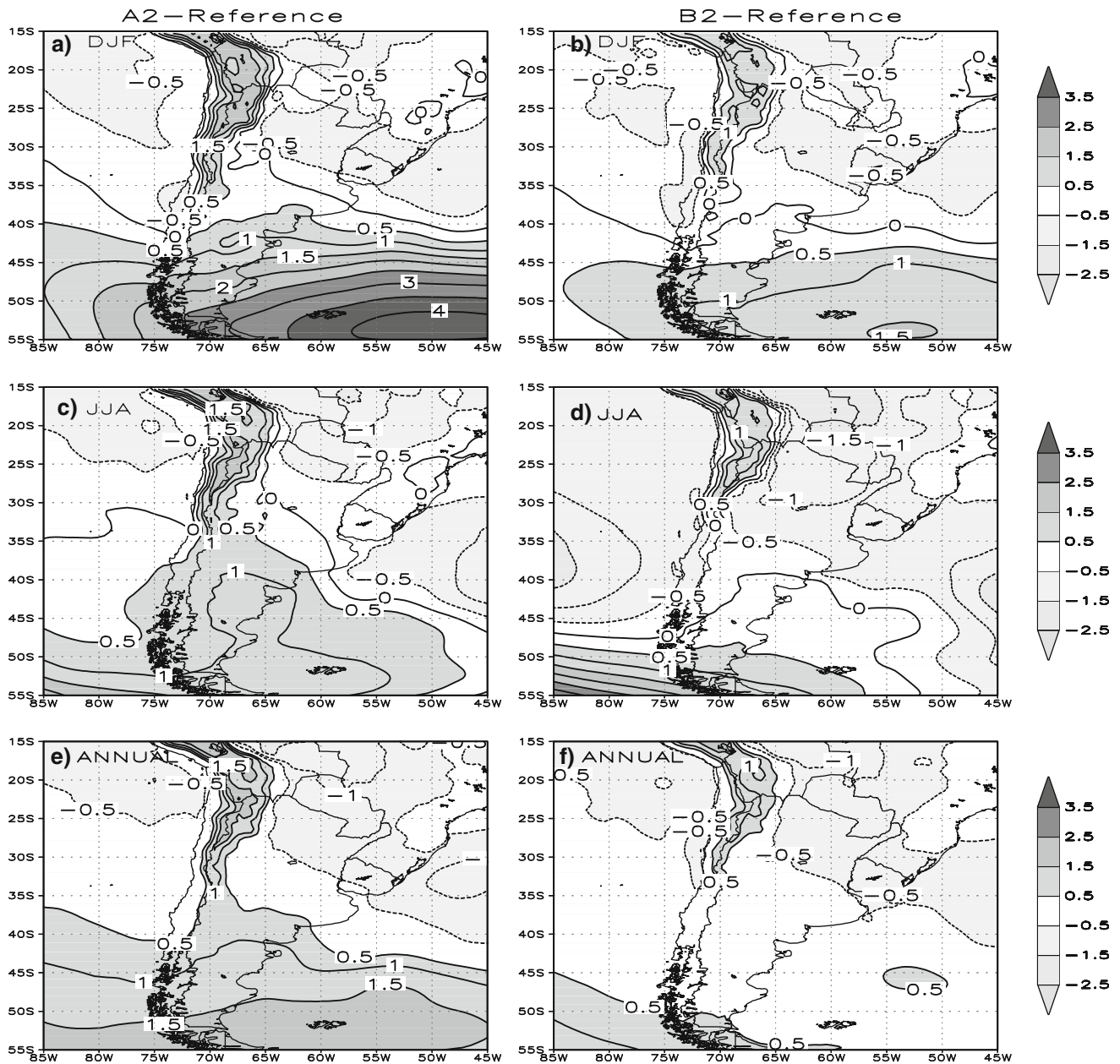


Fig. 2 Changes in 10-year summer, winter and annual mean sea level pressure for the A2 simulation (left) and the B2 simulation (right)

3.1.2 Surface air temperature

Changes in DJF, JJA and annual mean surface air temperature are shown in Fig. 4. Changes in mean temperature are statistically significant at a 95% confidence level for all seasons and both emission scenarios over the entire domain. For both scenarios the warming pattern is similar but with some qualitative and quantitative differences. The simulated changes in the annual mean temperature range between 2.5 and 4.5°C for the A2 and between 1.5 and 3.5°C for the B2 scenario. The warming is larger over

tropical and subtropical latitudes and weakens at higher latitudes. This feature is found in the annual mean change and for all seasons. The temperature increase over tropical and subtropical latitudes is larger during JJA compared with DJF, but the reverse pattern is found over higher latitudes. The warming in southern Brazil, Paraguay, Bolivia and northeastern Argentina during JJA reaches a maximum of 5.5°C for the A2 scenario and 4.5°C for the B2 scenario. Large warming is also simulated over the Andes region, mainly in the winter season. For DJF the maximum temperature increase is located over southern

MM5 GEOPOTENTIAL HEIGHT (500 hPa)

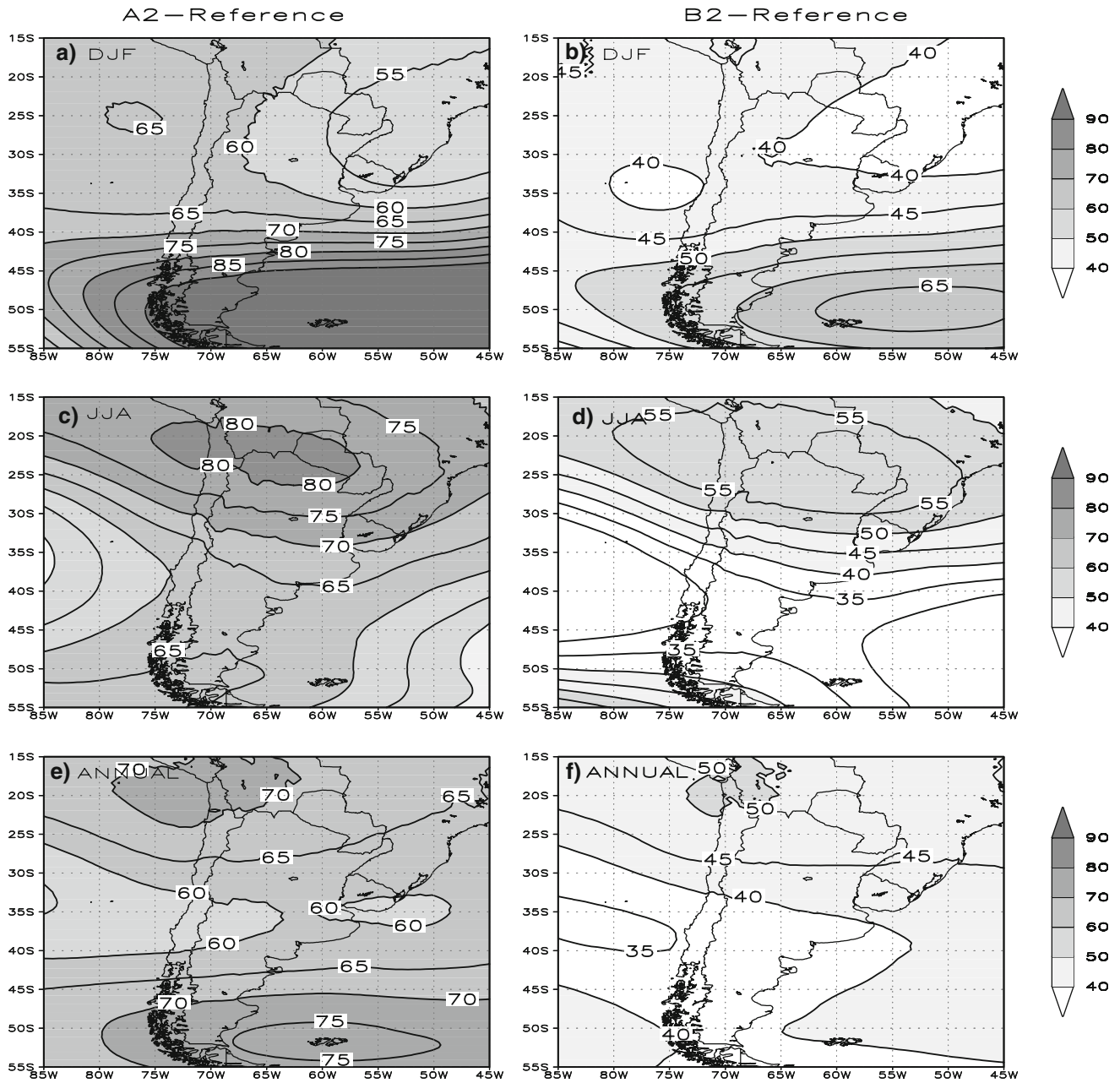


Fig. 3 Changes in 10-year summer, winter and annual mean 500 hPa geopotential height for the A2 simulation (*left*) and the B2 simulation (*right*)

Brazil. In Paraguay, southern Brazil and northern Argentina the warming peaks in spring when it locally reaches 6.0°C in the A2 scenario and 4.0°C in the B2 scenario (not shown). Over southern Argentina and Chile the warming reaches 2.5°C for the A2 scenario and less than 2.0°C for the B2 scenario and peaks mainly during the summer season.

Both simulations show a large increase in the maximum temperatures in northern Argentina, Paraguay, Bolivia and

southern Brazil, reaching 6.0°C in the A2 scenario (not shown). For minimum temperatures, both scenarios show the same spatial patterns as in the maximum temperatures, but the magnitude of the warming is reduced. The increase in minimum temperature peaks in spring reaching 5.0°C in a patch in southern Brazil for the A2 simulation (not shown).

The patterns of change in the surface air temperature field are broadly similar to those simulated by the

MM5 MEAN TEMPERATURE (C)

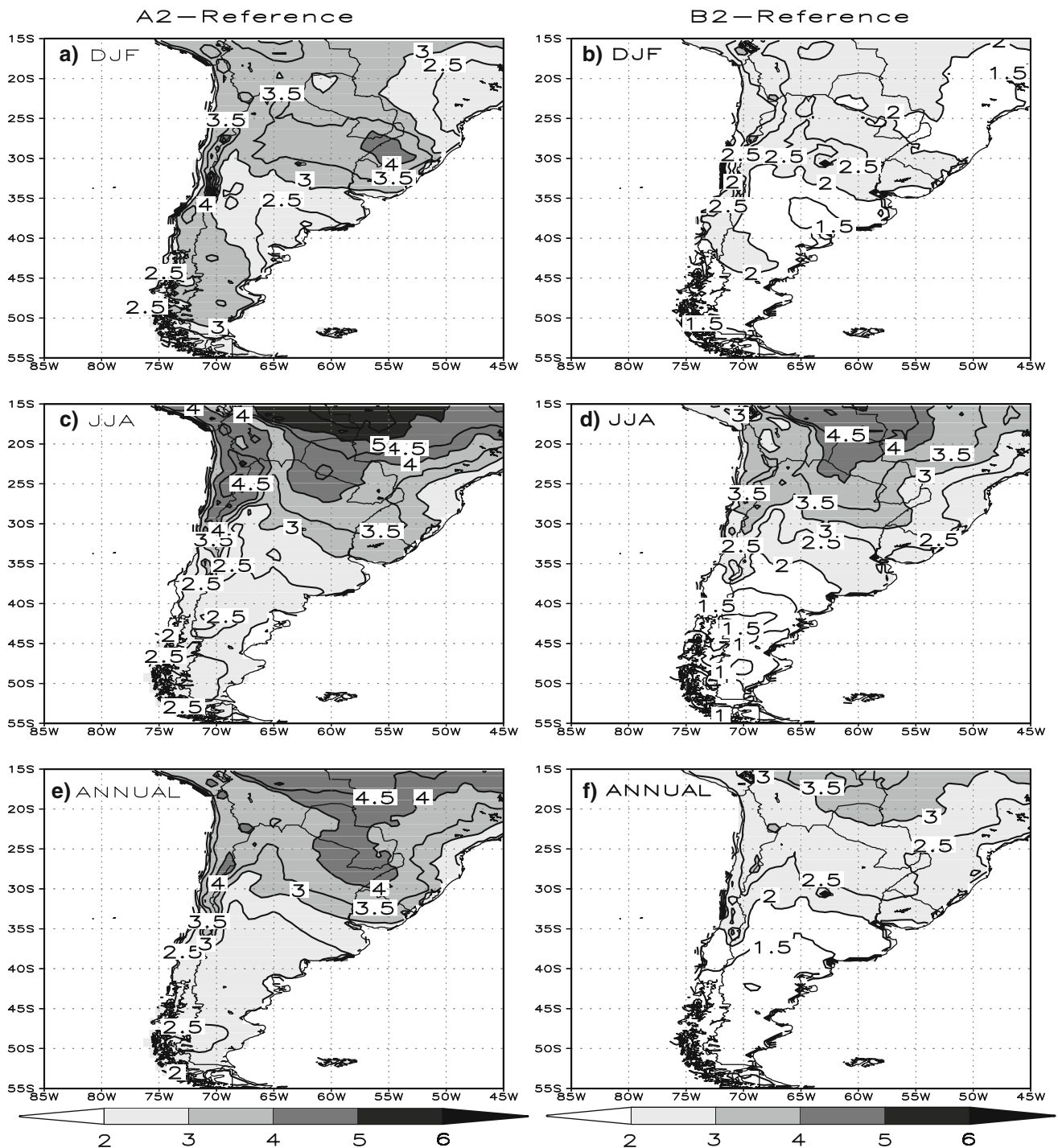


Fig. 4 Changes in 10-year summer, winter and annual mean temperature for the A2 simulation (*left*) and the B2 simulation (*right*)

HadAM3H model (not shown), though modulated by regional scale processes. An important aspect is the finer scale structure of the change signal associated with the topography. Moreover over the Andes the HadAM3H model projects a larger warming than the regional model. The difference between the two projections is around 2°C.

Comparing the projected changes under the A2 scenario between the HadAM3H model and the multi-model ensemble mean from Meehl et al. (2007), we found that both agree in terms of the spatial distribution and magnitude of the warming, except over the Andes where the HadAM3H model projects a larger warming. Overall, the

regional projection agrees better with the multi-model ensemble mean than with the driving model.

Taking into account the spatial pattern of the change in mean temperature, we have defined several sub-regions (Fig. 5) in order to evaluate the average changes in the seasonal cycle. Figures 6 and 7 show, for both climate change simulations, the seasonal cycles of the mean and the maximum and minimum temperature change over the sub-regions defined in Fig. 5, respectively. The figures also display the 95% confidence limit of significance for a two sided test. The simulated changes in temperatures are in most cases statistically significant.

The seasonal cycle of mean temperature change (Fig. 6) differs dramatically between northern and southern sub-regions. The largest warming in the ST region occurs in September (A2) and July (B2), and the smallest in February (A2) and May (B2). Over PAT, the largest warming is in summer (February, A2 and B2) and the smallest is in September (A2 and B2). Over CARG the annual cycle of change is qualitatively different for both emission scenarios, but large warming is evident for JJA. The SESA region shows a similar temperature change all over the

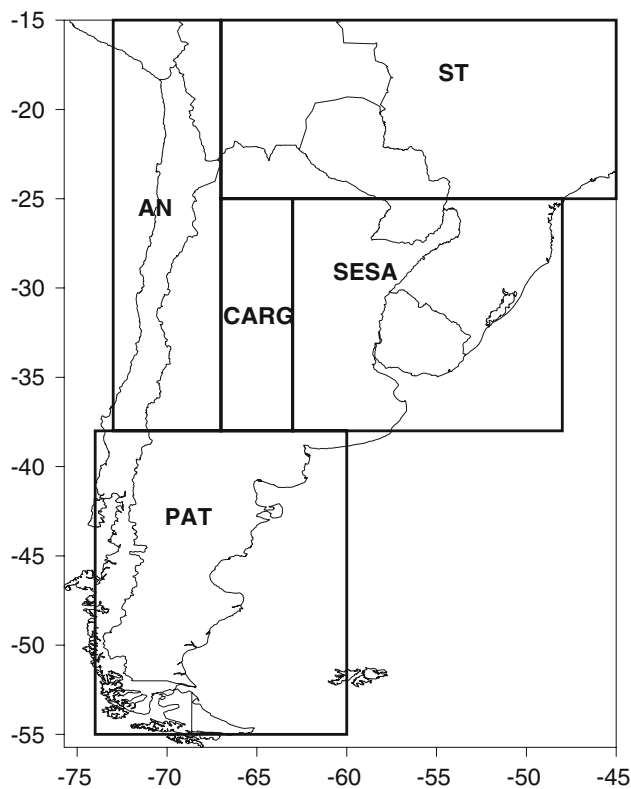


Fig. 5 Sub-regions used for a more detailed analysis of the annual cycle for mean, maximum and minimum temperatures. *ST* Subtropical; *AN* Andes; *CARG* Central Argentina; *SESA* South-eastern South America; *PAT* Patagonia

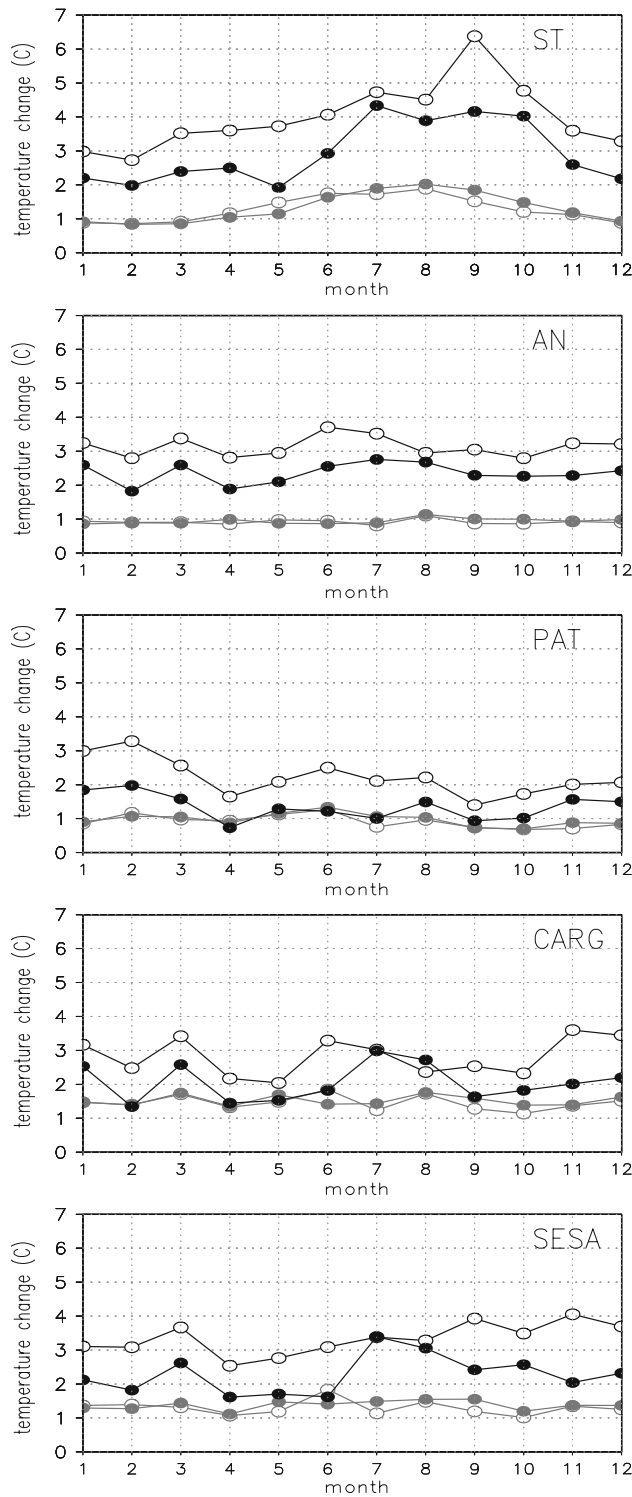
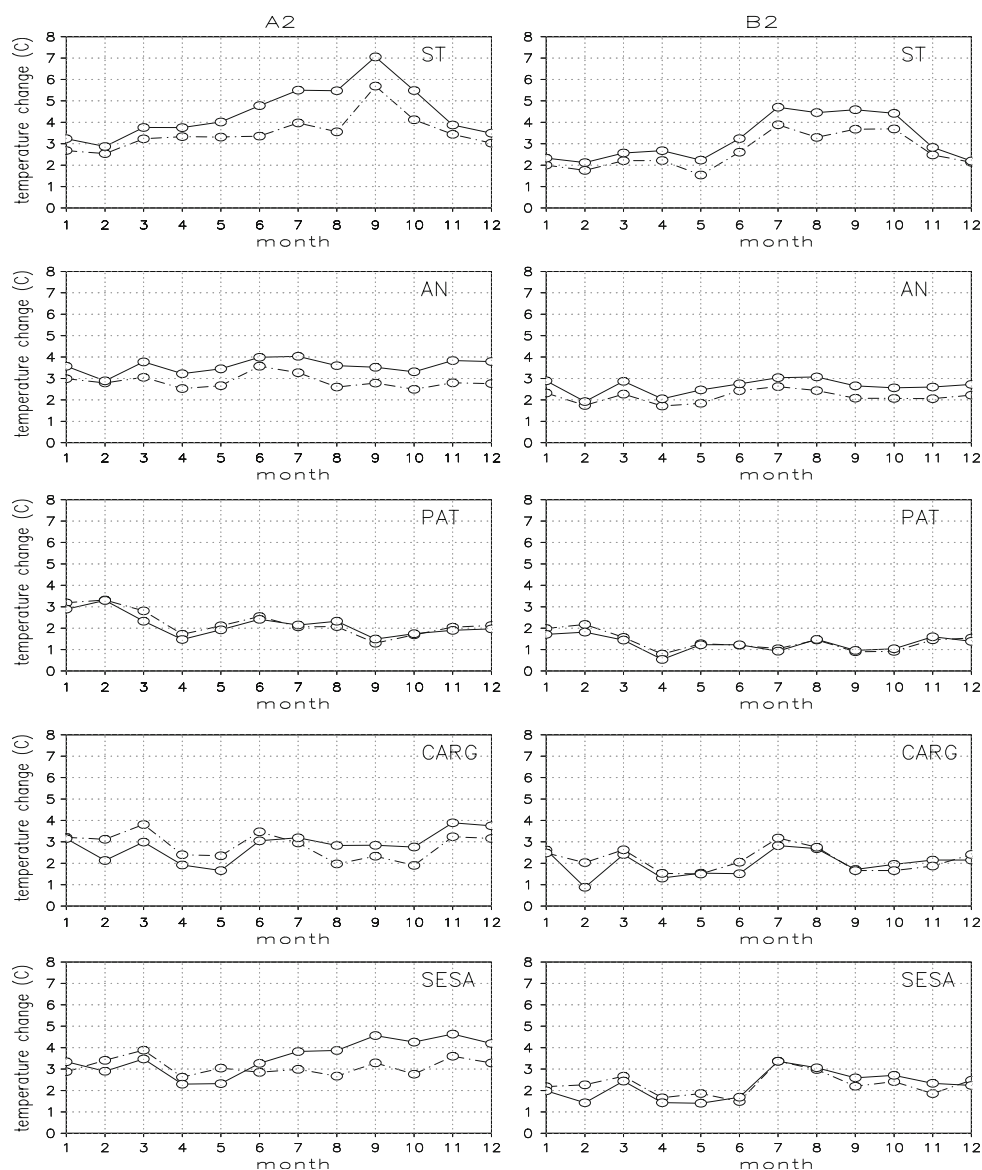


Fig. 6 Seasonal cycles of mean temperature changes averaged over the sub-regions of Fig. 5. The lines used for A2 simulation are identified with the *white circles* and the *black circles* are used for the B2 simulation. The *gray lines* indicate the 95% confidence interval for the mean temperature changes. *White circles* corresponds to the A2 simulation and *gray circles* to the B2 simulation

Fig. 7 Seasonal cycles of minimum temperature change (dashed lines) and maximum temperature change (solid lines) averaged over the sub-regions of Fig. 5 for the A2 (left panels) and the B2 (right panels) scenarios



year. In the AN region the largest warming occurs in winter (June–July) and the smallest in summer (February). The seasonal cycles of maximum and minimum temperature change (Fig. 7) are quite similar to the mean temperature change cycle with the largest warming in the ST region during September (A2) and July (B2), and the smallest in February (A2) and May (B2). In PAT, again the largest warming is in summer (February, A2 and B2) and the smallest is in April (A2 and B2). The changes in maximum temperature are larger than the changes in the minimum temperature, particularly in the ST and the AN regions.

3.1.3 Precipitation

The changes in DJF, JJA and annual mean precipitation are shown in Fig. 8. There are large seasonal and geographical

variations in the change, and also some substantial differences between A2 and B2. Like temperature and sea level pressure, precipitation changes generally less in the B2 than in the A2 simulations, but mostly to the same direction. However, some qualitative differences between the two forcing scenarios also occur.

The A2 scenario simulation shows a significant decrease in annual precipitation in the southern Andes and a broad area of precipitation increase over central Argentina. Changes in the precipitation amount along the coast of Chile for JJA are consistent with the poleward expansion of the South Pacific subtropical high and the associated poleward shift of the Pacific Ocean storm-track, inducing a significant decrease in precipitation over central Chile and an increase in precipitation over southern Chile and southern Argentina. The patterns of precipitation change from the regional

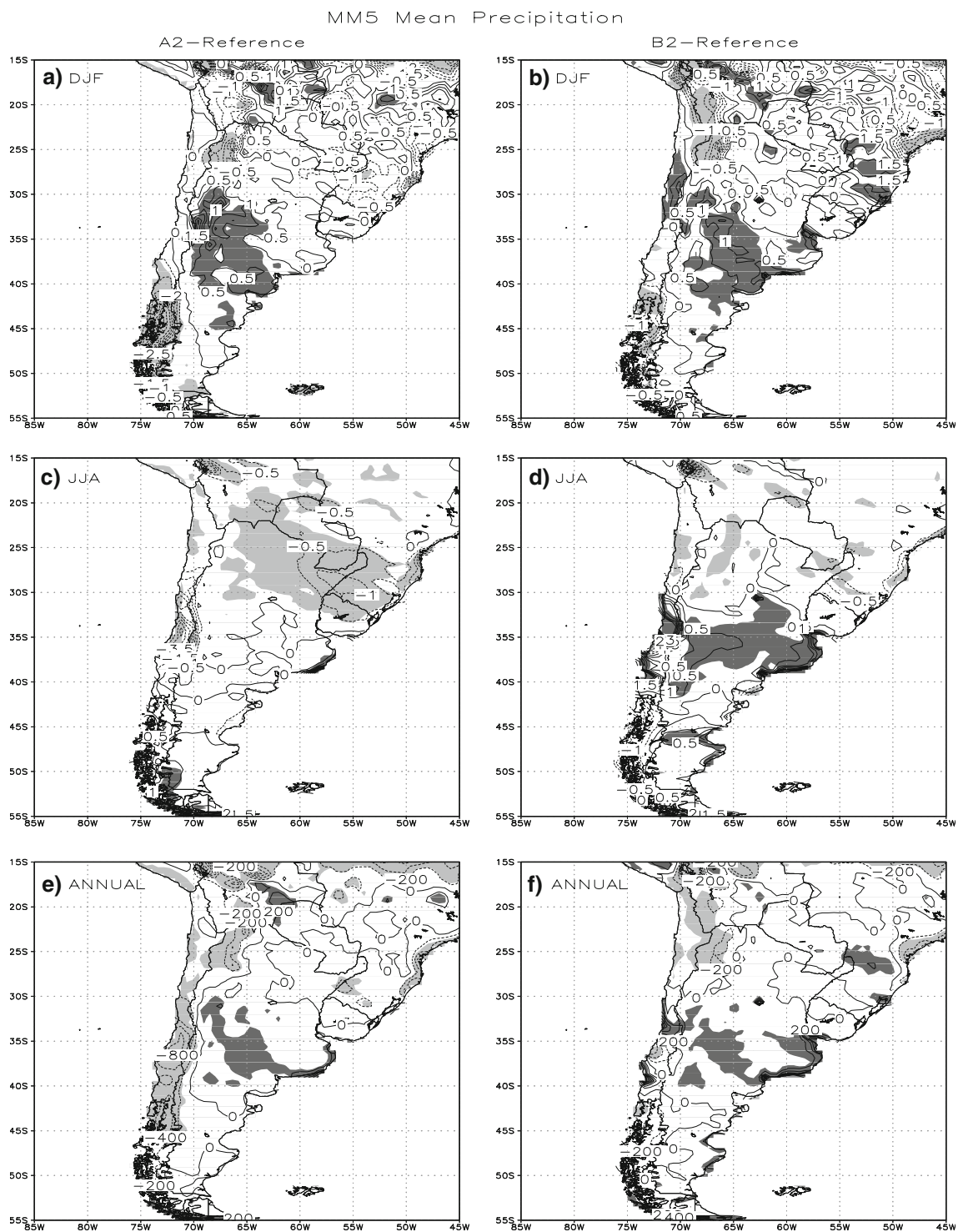


Fig. 8 Changes in 10-year DJF, JJA and annual mean precipitation for the A2 simulation (*left panels*) and the B2 simulation (*right panels*). DJF and JJA precipitation change in mm/day (contoured each 0.5 mm/day) and annual precipitation change in mm (contoured each

200 mm). *Light (dark) shading* indicates areas where the precipitation decrease (increase) is statistically significant at a 90% confidence level

simulations are broadly similar to those from the HadAM3H model (not shown), except in the southern tip of South America where the HadAM3H model projects dryer conditions. Moreover, the regional model agrees better with the

multi-model ensemble mean shown in Meehl et al. (2007). The projected changes over the western coast of South America are mostly in the same direction as the observed tendencies during the last 40 years (Ciappesoni et al. 2005).

The regional simulation for the A2 scenario shows a widespread significant increase in precipitation during DJF over central Argentina, which is consistent also with the projected change in HadAM3H. This increase in precipitation is mostly due to the regional increase of the cyclonic circulation referred to as the Chaco low, in tandem with a poleward shift of the subtropical anticyclone over the Atlantic, which induce enhanced moisture transport towards the central plains of Argentina. This pattern of change also agrees with the results from the multi-model ensemble mean shown in Meehl et al. (2007) for the SRES A1B scenario.

The regional model shows a significant decrease in precipitation over the Altiplano region (western Bolivia) during summer months. However, in the HadAM3H model the decrease in precipitation over that area is much weaker. Another remarkable feature is the significant decrease in precipitation for the A2 scenario during JJA over south-eastern South America in agreement with the HadAM3H projection.

The main differences between the A2 and the B2 scenarios are detected during winter months. In particular, the regional model projects for the B2 scenario an increase of precipitation over central Argentina and central Chile and a decrease over the southern coast of South America. The same differences between the two scenarios are present in the HadAM3H model. This reflects different changes in the atmospheric circulation for both scenarios.

In summary, a comparison between the pattern of change in the precipitation field simulated by the regional and the HadAM3H models suggests that, as for the temperature changes, the regional model produces climate change patterns with greater spatial detail due to regional processes involving topographic features, which are better resolved by the high resolution model. Major discrepancies between the changes produced by the regional model and the driving model are apparent mainly over the Andes, mostly due to the representation of this topographic feature, which is smoothed, in terms of being less steep and lower in the HadAM3H model compared with the regional model.

The annual cycles of the seasonal mean precipitation for present climate, the A2 and the B2 scenarios averaged over the sub-regions of Fig. 9 are summarized in Fig. 10. The statistical significance of the changes for both the A2 and the B2 scenarios at the 90% confidence level is also displayed. We focus the discussion mainly on significant changes of the seasonal mean precipitation. Over the Central Andes (CA) and the Altiplano (AL) regions the mean precipitation decreases for both the A2 and the B2 simulations for all seasons. For the Subtropical Andes region (SUA), there is a decrease in precipitation during March–April–May (MAM), JJA and September–October–November

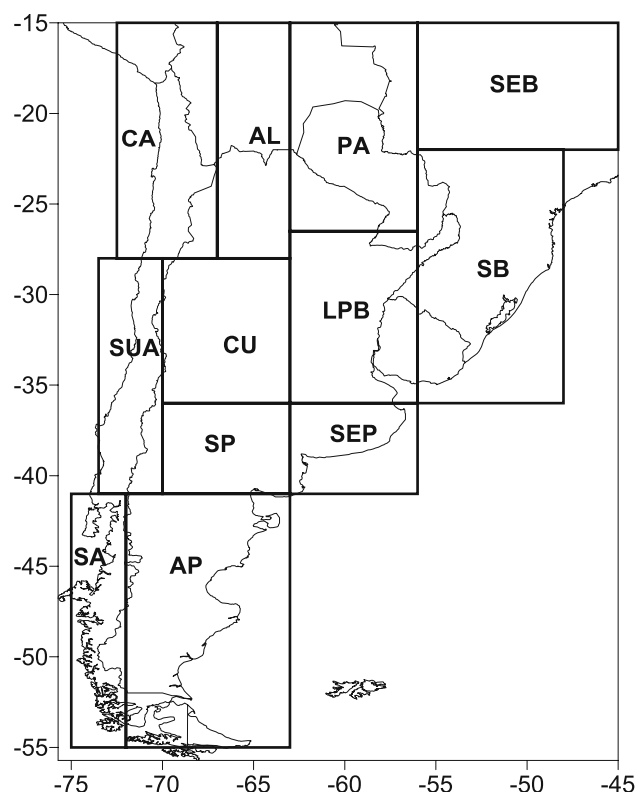


Fig. 9 Sub-regions used for a more detailed analysis of the annual cycle for precipitation. CA Central Andes; AL Altiplano; PA Paraguay; SEB South-eastern Brazil; SUA Subtropical Andes; CU Cuyo; LPB La Plata Basin; SB Southern Brazil; SP Southern Pampas; SEP South-eastern Pampas; SA Southern Andes; AP Argentinean Patagonia

(SON) for A2. It is important to remark that the largest precipitation decrease is projected for the rainy season. As mentioned previously the precipitation change for the B2 scenario shows an increase mainly during JJA and SON. In Southern Andes (SA) the mean precipitation decreases significantly only during DJF for the A2 scenario.

The mean precipitation in La Plata Basin (LPB) increases during MAM and decreases during JJA for the A2 scenario. This indicates that the regional projection predicts a wetter rainy season and a drier dry season. Over Southern Brazil (SB) the most significant changes are a precipitation decrease during JJA for both the A2 and B2 scenarios and an increase during MAM. In Paraguay (PA) precipitation decreases substantially during JJA only for the A2 scenario. Over South-eastern Brazil (SEB) significantly dryer conditions are projected under the A2 scenario for MAM. In Cuyo (CU) the mean precipitation increases in the first half of the year in both simulations, though this increase is significant only during DJF for the A2 scenario. In South-eastern Pampas (SEP) the mean precipitation increases for all seasons in both simulations, with larger increases for B2 compared with A2.

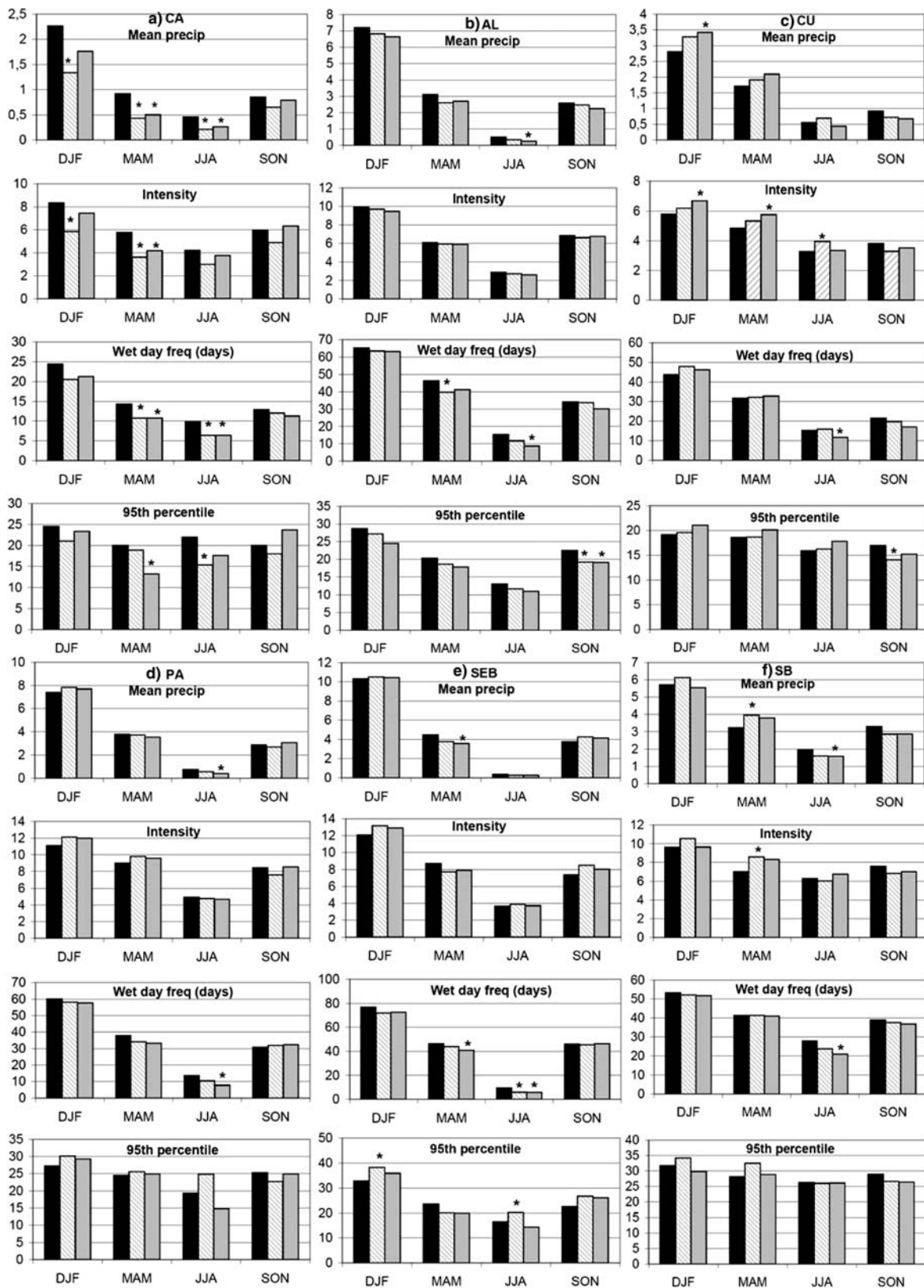


Fig. 10 Seasonal mean precipitation (mm/day), intensity (mm/day), wet day frequency (days) and 95th percentile (mm) averaged over the sub-regions defined in Fig 9. Black bars for present climate simulation, dashed bars and light grey bars for the B2 and the A2 scenarios,

respectively. Asterisks denote cases in which the difference between the corresponding scenario (B2 and A2, respectively) and present conditions is statistically significant at the 90% confidence level

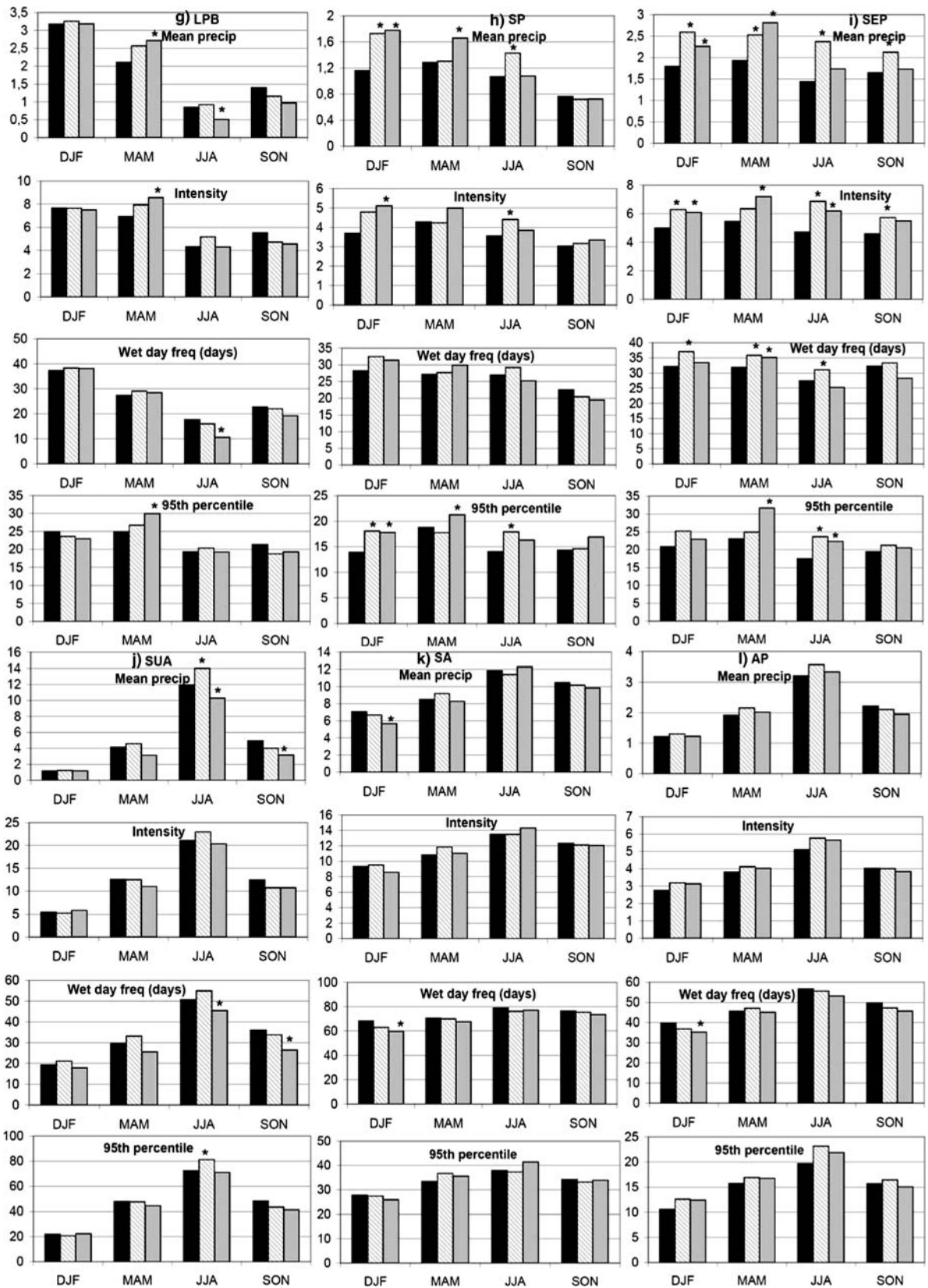


Fig. 10 continued

3.2 Changes in daily precipitation statistics

In order to have a more complete picture of the nature of the precipitation changes described above, we analyze here the changes in some basic high-frequency precipitation statistics. We focus our analysis on the changes in wet day frequency, precipitation intensity and extreme precipitation events. Wet day frequency was calculated as the number of days per season with rainfall amounts greater than 0.1 mm. Extreme precipitation events in this study are represented by the 95th percentile of daily precipitation. A threshold of 0.1 mm day^{-1} is used to select rain days for the estimation of the 95th percentile. Precipitation intensity is calculated as the seasonal mean precipitation rate computed for wet days.

The statistical significance of the changes in intensity, wet day frequency and extreme events, was evaluated in terms of the signal-to-noise ratio. The seasonal mean climate change signal for each region (computed as the difference between the climates in the scenario simulation and the present climate simulation) was compared with the interannual variability, as a measure of noise. The extent to which the signal-to-noise ratio is large enough (significantly larger than 1) was tested using the Student's *t*-test (Hayashi 1982).

Figure 10 shows the seasonal mean intensity, the 95th percentile and the wet-day frequency, for present climate, A2 and B2 scenarios for all regions based on the regional simulations. Over the CA region (Fig. 10a), the precipitation decrease is due to a decrease in both the number of rainy days and the intensity of rainfall. Note that the largest decrease in precipitation is estimated for DJF and MAM, when the mean rainfall is larger. Over SEB (Fig. 10e), where changes in the mean precipitation amounts are relatively small in all seasons, it is interesting to note that the number of rainy days is reduced for both scenarios but the intensity and the 95th percentile increases, mainly during DJF and SON, the rainy seasons for this region. A similar behaviour is found over the PA region (Fig. 10d). Over the SB region (Fig. 10f) the mean precipitation increase for MAM is mostly due to the increase in the precipitation intensity, rather than in the number of rainy days. Accordingly, the extreme precipitation events are expected to be more intense. This behaviour is also revealed in the increase of the 95th percentile. Over the LPB region (Fig. 10g), the most interesting feature is the increase in precipitation during MAM, due to the increase in intensity, consistently associated with a substantial increase in the extreme events. This is a remarkable feature because the increase is mainly during the season when maximum rainfall occurs. This result is consistent with the increase in moisture convergence over the region in the scenario

simulations associated mainly with more intense northerlies over northern Argentina. On the other hand, a substantial decrease in precipitation during JJA for the A2 scenario is mostly due to a decrease in the number or rainy days. The southward shift of the south Pacific Ocean storm-track and the poleward extension of the subtropical anticyclone over the Atlantic may reduce the cyclonic activity over subtropical latitudes, which is the main mechanism associated to rainfall during winter months over that region. In the SEP region (Fig. 10i), not only the mean precipitation increases for all seasons in both scenarios, the intensity increases strongly with a moderate increase or even a decrease in the frequency of wet days. The associated mechanisms are strongly related to the changes in the circulation. During summer months, the enhanced poleward moisture flux, associated with the southward displacement of the subtropical anticyclone over the Atlantic Ocean is one of the main mechanisms. On the other hand, during winter, due to the poleward shift of the Pacific storm-track, the cyclones developing over the Pacific Ocean reach the Andes at higher latitudes, where the mountains are lower. In consequence, the path of the systems once they are located downstream of the orographic barrier will have a more zonal trajectory, instead of deflecting northward, as they do when they impinge the topography at lower latitudes (Gan and Rao 1994; Vera et al. 2002). Over the SP region (Fig. 10h) there is an overall increase in precipitation in all seasons mainly due to increases in the intensity. Over the SUA region (Fig. 10j) the regional model projects for the A2 scenario a decrease in precipitation for MAM, JJA and SON, mainly associated with a decrease in the number of rainy days. This result is consistent with projections from coupled general circulation models (Sun et al. 2007) and it is associated with the poleward shift of the Pacific storm-track and southward extension of the subtropical high over the Pacific Ocean. Over the SA region (Fig. 10k) the decrease in the mean precipitation during summer is mainly associated to a decrease in wet day frequency. This is consistent with the weakening of the westerlies mentioned previously. During JJA the increase in precipitation is mostly due to the increase in the intensity.

We mostly find that over subtropical latitudes, increases in the mean precipitation during summer and intermediate seasons are mainly associated with increasing intensity, and consistently increasing extreme events, whereas changes in the frequency of rain are small. On the other hand, over regions where a decrease in the mean precipitation is projected this is mostly due to a decrease in the number of rainy events. Overall, the general characteristics of the projected changes are also consistent with reported changes over the past 30 years (Barros et al. 2000; Haylock et al. 2006; Nuñez et al. 2007).

4 Summary and conclusions

This paper presents the results from regional simulations of climate change under two IPCC emission scenarios (A2 and B2) for the period 2081–2090 over southern South America. We analyzed the projected climatic changes with respect to the reference period 1981–1990. The simulations were performed with the MM5 regional climate model nested within a high resolution version of the Hadley Centre Global Atmospheric Model (HadAM3H). The focus was on the changes in the mean circulation and surface variables, in particular, surface air temperature and precipitation. Changes in daily precipitation statistics were also analyzed in order to understand the nature of the precipitation changes. Our primary conclusions can be summarized as follows:

1. In all seasons, southern South America undergoes a warming in both the A2 and the B2 scenarios. The warming is in the range of 1.5–5.5°C for A2 and 1–4°C for B2. Maximum changes in the mean temperature are projected for tropical and subtropical regions and minimum changes are projected for higher latitudes (south of 35°S). Over tropical and subtropical regions the maximum increase is mainly during spring and over higher latitudes the maximum warming is projected during summer.
2. The patterns of change in the maximum and the minimum temperatures are similar to the mean temperature. Nevertheless, changes are larger for the maximum temperature than for the minimum temperature particularly over tropical and subtropical regions.
3. The precipitation changes vary substantially from season to season and across regions in response to changes in the large scale circulation. An increase in precipitation in central Argentina is projected for the summer and the fall seasons (in the west and in the humid Pampas precipitation increases by up to approximately 180 mm per season in the A2 simulation). This is mostly due to enhanced moisture flux from the north, associated with the enhancement of the cyclonic circulation over northern Argentina (the Chaco low) and the southward extension of the subtropical highs. The change in the mean precipitation is reversed during JJA over southeastern South America, mainly due to the poleward shift of the subtropical anticyclone over the Atlantic Ocean and the poleward shift of the storm-track over the Pacific Ocean, which reduces the cyclonic activity over the region. A substantial decrease in precipitation is also projected over the western coast of South America, mainly during JJA associated with a poleward shift of the Pacific storm-track.

We mostly find that over subtropical latitudes, increases in mean precipitation during summer and intermediate seasons are mainly associated with increasing intensity, and consistently increasing extreme events, whereas changes in the frequency of rain are small. On the other hand, over regions where a decrease in mean precipitation is projected this is mostly due to a decrease in the number of rainy events. Overall, the projected changes are also consistent with reported changes over the past 30 years (Barros et al. 2000; Haylock et al. 2006).

The precipitation intensity increases almost over all regions in southeastern South America, mainly during the rainy season, even over regions where the mean precipitation remains unchanged. Accordingly, extreme precipitation events also increase. The changes in the frequency of rainy days vary substantially over regions and seasons, depending on the mechanisms associated with the precipitation changes.

4. The B2 simulation shows a similar geographical pattern of the changes in temperature as the A2 simulation. The precipitation pattern of change presents large quantitative and qualitative differences between the two emission scenarios.
5. The broad patterns of change in the nested regional climate model MM5 and driving HadAM3H fields are generally consistent each other, as can be expected from the strong influence of the boundary forcing on the regional model simulation. The largest differences between the two models in the temperature and precipitation changes are evident close to the Andes.

The results reported here are based on one realization forced by a single driving model. Due to the lack of other regional simulations over the region, it is difficult to evaluate the robustness of the projected changes, though they are consistent with the driving model projections. However, there are some differences in the projected changes between the HadAM3H and the MM5 models. We have found that the regional model agrees better with the multi-model ensemble mean results reported in Meehl et al. (2007) suggesting the added value of the regional simulation. It is hoped that other regional climate change simulations be conducted in order to gain understanding on the uncertainties of the regional projections discussed.

Acknowledgments This work was supported by the UBACYT Grant 01-X264, ANPCYT Project PICT2005 32194 and partially by EU CLARIS Grant. We would like to thank the Hadley Centre for providing the HadAM3H data. The authors wish to thank to anonymous reviewers whose insightful comments and suggestions led to improve the manuscript. We also thank Alfredo Rolla for his invaluable cooperation in running the model.

References

- Barros VR, Castañeda ME, Doyle ME (2000) Recent precipitation trends in southern South America east of the Andes: An indication of climatic variability. In: Smolka PP, Volkheimer W (eds) Southern Hemisphere Paleo-and Neoclimates. Key sites, methods, data and models. Springer, Berlin, pp 187–206
- Christensen JH, Carter TR, Rummukainen M, Amanatidis G (2007) Evaluating the performance and utility of regional climate models: the PRUDENCE project. *Clim Change* 81:1–6. doi: [10.1007/s10584-006-9211-6](https://doi.org/10.1007/s10584-006-9211-6)
- Ciappesoni HH, Fernández AE, Nuñez MN (2005) Impactos de la urbanización y de los cambios en el uso de la tierra en Argentina. CD Anales IX Congreso Argentino de Meteorología (CONGR-EMET IX), 9 páginas, ISBN 987-22411-0-4
- Gan M, Rao V (1994) The influence of the Andes Cordillera on transient disturbances. *Mon Weather Rev* 122:1141–1157. doi: [10.1175/1520-0493\(1994\)122<1141:TIOTAC>2.0.CO;2](https://doi.org/10.1175/1520-0493(1994)122<1141:TIOTAC>2.0.CO;2)
- Grell GA, Dudhia J, Stauffer DR (1993) A description of the fifth-generation Penn System/NCAR Mesoscale Model (MM5). NCAR Tech Note NCAR/TN-398+1A, 107 p
- Hayashi Y (1982) Confidence intervals of a climatic signal. *J Atmos Sci* 39:1895–1905. doi: [10.1175/1520-0469\(1982\)039<1895:CIOACS>2.0.CO;2](https://doi.org/10.1175/1520-0469(1982)039<1895:CIOACS>2.0.CO;2)
- Haylock MR, Peterson TC, Alves LM, Ambrizzi T, Anunciação YM, Baez J et al (2006) Trends in total and extreme South American rainfall in 1960–2000 and links with sea surface temperature. *J Clim* 19:1490–1512. doi: [10.1175/JCLI3695.1](https://doi.org/10.1175/JCLI3695.1)
- IPCC (2000) Emission scenarios, a special report of working group III of the intergovernmental on climate change. Nakicenovic N Coordinating Lead Author. Cambridge University Press, Cambridge, p 599
- Jones RG, Murphy JM, Hassell D, Taylor R (2001) Ensemble mean changes in a simulation of the European mean climate of 2071–2100 using the new Hadley Centre regional modeling system HadAM3H/HadRM3H. Hadley Centre Report, p 19
- Mearns et al (2005) NARCCAP (North American Regional Climate Change Assessment Program). A multiple AOGCM and RCM climate scenario project over North America. In: AMS 16th conference on climate variations and change, pp 235–238
- Meehl GA, Stocker TF, Collins WD, Friedlingstein P, Gaye AT, Gregory JM et al (2007) Global climate projections. In: Solomon S, Qin D, Manning M, Chen Z, Marquis M, Averyt KB, Tignor M, Miller HL (eds) Climate change 2007: the physical science basis. Contributions of Working Group I to the Fourth Assessment Report of the Intergovernmental Panel on Climate Change. Cambridge University Press, Cambridge
- Nuñez MN, Ciappesoni HH, Rolla A, Kalnay E, Cai M (2007) Impact of land-use and precipitation changes on surface temperature trends in Argentina. *J Geophys Res* (in press)
- Pope VD, Gallani ML, Rowntree PR, Stratton RA (2000) The impact of new physical parameterizations in the Hadley Centre climate model. *Clim Dyn* 16:123–146. doi: [10.1007/s003820050009](https://doi.org/10.1007/s003820050009)
- Solman S, Nuñez M, Cabré MF (2008) Regional climate change experiments over southern South America. I: present climate. *Clim Dyn* 30:533–552. doi: [10.1007/s00382-007-0304-3](https://doi.org/10.1007/s00382-007-0304-3)
- Sun Y, Solomon S, Aiguo D, Portman RW (2007) How often will it rain? *J Clim* 20:4801–4818. doi: [10.1175/JCLI4263.1](https://doi.org/10.1175/JCLI4263.1)
- Vera CS, Vighiarolo PK, Berbery H (2002) Cold season synoptic scale waves over subtropical South America. *Mon Weather Rev* 130:684–699. doi: [10.1175/1520-0493\(2002\)130<0684:CSSSWO>2.0.CO;2](https://doi.org/10.1175/1520-0493(2002)130<0684:CSSSWO>2.0.CO;2)
- Whetton PH, Katzfey JJ, Hennessy KJ, Wu X, McGregor JL, Nguyen KC (2001) Developing scenarios of climate change for South-eastern Australia: an example using regional climate model output. *Clim Res* 16:181–201. doi: [10.3354/cr016181](https://doi.org/10.3354/cr016181)